Supporting Information

Ultrahigh-Energy-Density Sorption Thermal Battery Enabled by Graphene Aerogel-based Composite Sorbents for Thermal Energy Harvesting from Air

Taisen Yan[1,‡], Tingxian Li[1,‡,], Jiaxing Xu[1], Jingwei Chao[1], Ruzhu Wang[1,]*, Yuri I. Aristov[3], Larisa G. Gordeeva[2], Pradip Dutta, S. Srinivasa Murthy[4]*

[1] Research Center of Solar Power & Refrigeration, School of Mechanical Engineering, Shanghai Jiao Tong University, Shanghai, 200240, China

[2] Boreskov Institute of Catalysis, Russian Academy of Sciences, Lavrentiev Av, Novosibirsk 630090, Russia

[3] Department of Mechanical Engineering, Indian Institute of Science, Bangalore 560012, India

[4] Interdisciplinary Centre for Energy Research, Indian Institute of Science, Bangalore 560012, India

[‡] These authors contributed equally to this work.

*Correspondence and requests for materials should be addressed to T.X. Li (email: Litx@sjtu.edu.cn) or to R.Z. Wang (email: Rzwang@sjtu.edu.cn).

S1. Experimental Procedure

Chemicals and materials

Natural flake graphite with 325 mesh was purchased from XFNANO Co. Ltd. Chemicals, including $NaNO_3$, $KMnO_4$, H_2SO_4, HCl, 30% H_2O_2, Vitamin C, alkyl polyglucoside (50 wt%) and $CaCl_2$, were purchased from Sinopharm Chemical Reagent Co., Ltd.

Preparation of graphene oxide (GO)

GO was prepared by a modified Hummer method.[1] In brief, 3.0 g of nature flake graphite was added to 144.0 mL concentrated sulfuric acid, followed by slowly adding 3.0 g sodium nitrate and 18.0 g potassium permanganate in an ice bath for 30 min. Then, the mixture was continuously stirred at 35 ^{o}C for 8 h, forming a thick paste. After oxygenation, 200.0 mL de-ionized water and 10 mL 30% H_2O_2 were added into the mixture, turning the color of the solution from brown to yellow. The mixture was filtered and washed with 250.0 mL HCl aqueous solution to remove metal ions, followed by repeatedly washed with water and centrifuged at 10000 rpm for 1 h to remove the acid. Then, mild sonication (100 W, 30 min) was used to exfoliate the graphite oxide to obtain a GO suspension. And low speed centrifugation was done at 3000 rpm for 10 min to remove thick multilayer flakes. Finally, the obtained dispersion liquid was freeze dried to obtain the graphene oxide powder.

Preparation of composite sorbent

Graphene aerogel (GA) is fabricated through chemical reduction.[2-3] Firstly, 100.0 mL aqueous suspensions of graphene oxide (GO) prepared by a modified Hummer method at a concentration of 10.0 $mg \cdot mL^{-1}$ with 2.0 g vitamin C and 2.0 g alkyl polyglucoside are mixed. Secondly, the mixture is sealed into a glass dish and heated at 80 ºC for 8 h to synthesize graphene hydrogel (GH). Afterwards, the synthesized GH is washed with deionized water several times. Thirdly, the prepared GH is frozen completely by liquid nitrogen and dried for 24 h to gain graphene aerogel (GA). Finally, the impregnation of calcium chloride ($CaCl_2$) into GA matrix is performed by immersing the GA into the aqueous salt solution with different concentrations between 20 wt%~40 wt% for 24 h. The wet $CaCl_2$@GA composite sorbents are washed with deionized water to remove the residual salt on the surface of GA matrix and then dried at 80 ºC. According to the different concentrations of salt solution impregnated, the prepared composite sorbents are named as $CaCl_2$@GA_20, $CaCl_2$@GA_30, and $CaCl_2$@GA_40, respectively.

Characterization of composite sorbent

The $CaCl_2$@GA composite sorbents are characterized by X-ray photoelectron spectroscopy (AXIS Ultra DLD) using a monochromatic Al-Kα X-ray source. The morphologies of the composite sorbents are observed by a scanning electron microscopy (TESCAN-MAIA3).

Water sorption of composite sorbent

The water sorption/desorption tests are performed using a thermogravimetric analyzer (STA 449C, Netzsch) equipped with a moisture humidity generator (MHG 32,

ProUmid). The $CaCl_2$@GA samples are firstly kept at a constant temperature and humidity (humidity ranging from 30% RH to 90% RH at 30 ^oC) for 10 h to reach sorption equilibrium. Afterwards, the $CaCl_2$@GA samples are heated at 80 ^oC for 4 h to desorb water vapor. The sample temperatures are switched between 30 ^oC and 80 ^oC to conduct repeated water sorption-desorption cycles.

The water sorption equilibrium curves are measured by both a self-constructed water sorption system and an accelerated surface area and porosimetry system (ASAP) with addition of a water vapor generator. Isobaric equilibrium lines at different pressures (1200 Pa, 2500 Pa, 3000 Pa, and 4200 Pa) are tested within a temperature range of 10-90 ^oC. The isothermal equilibrium line is conducted at 25 ^oC with RH conditions ranging from 0-80% RH.

S2. Water sorption equilibrium experiments by self-constructed water sorption system

Water sorption equilibrium, including isothermal equilibrium curve and isobaric equilibrium curve, can be obtained by self-built sorption device. The isothermal equilibrium test procedures included: i) preparation step: put the sorbent into the sample chamber and set chamber temperature to regeneration temperature, then use a vacuum pump to degas the sample chamber and gas vessel to less than 1 Pa for 6 h. Then wait for the sample temperature stable. ii) adsorption step: Close valve 1 and open valve 3 to connect the evaporator and gas vessel, set the gas vessel to sorption vapor pressure. Then close valve 3 and open valve 1 to connect the sample chamber and gas vessel, wait

for the sample to reach equilibrium status, then the adsorption amount can be calculated by equations (S1-S2). Repeat adsorption step by increasing the relative humidity from 0.0% to 80.0% step by step. The isobaric equilibrium test is carried out at a series of sorption pressures, like 1200 Pa, 2500 Pa, 3200 Pa, 4200 Pa, at the temperature ranging from 90 ºC to 10 ºC. Test procedures included: i) preparation step: sample is put into the sample chamber and set the chamber to regeneration temperature, then use a vacuum pump to degas sample chamber and gas vessel to less than 1 Pa for 2 h, and set the chamber and gas vessel vapor pressure to sorption pressure. ii) adsorption step driving by decreasing the sorption temperature step by step.

$$\Delta m_s = \Delta m_{SC} + \Delta m_{GV} = \frac{\Delta p_{SC} \cdot V_{GV}}{R \cdot T_{GV}} + \frac{\Delta p_{GV} \cdot V_{SC}}{R \cdot T_{SC}} \tag{S1}$$

$$q = q_0 + \sum_{n=0}^{N} \frac{\Delta m_s}{m_{s,dry}} \tag{S2}$$

Where Δm_s (g) is the water mass adsorbed by sorbent. Δm_{SC} (g) and Δm_{GV} (g) are the water mass change in the sample chamber and gas vessel respectively. q ($g \cdot g^{-1}$) is the specific uptake, $m_{s,dry}$ (g) is the sorbent mass at dried state.

The reaction equilibrium for chemical reaction and solution absorption can be calculated based on the following equation,

$$\ln \frac{P_{vapor}}{P_0} = \frac{\Delta H_r}{RT} - \frac{\Delta S_r}{R} \tag{S3}$$

Where P_{vapor} (Pa) is the vapor pressure. P_0 (Pa) is the saturated vapor pressure at the

sorbent temperature. $\triangle S_r$ ($J \cdot mol^{-1} \cdot K^{-1}$) is the reaction entropy. $\triangle H_r$ ($kJ \cdot mol^{-1}$) is the reaction enthalpy. Based on the isobaric equilibrium curves of *Ln(P)* vs. *-1/T* at different water uptakes, the hydration-dehydration enthalpy of sorbent per mole of water at different water uptakes are obtained.

S3. Mathematical model for STB

The STB is composed of layer-by-layer sorbent sheets. To improve the mass and heat transfer of sorbents, forced air flow is used to enhance the desorption-sorption kinetics by improving the water vapor diffusion at the external surface of the sorbent. The water vapor from bulk gas diffuses into the sorbent layer through (i) external surface diffusion from bulk gas into the external surface of GA, (ii) intra pore diffusion from the external surface of GA to intra pore surface within the GA, and (iii) the hydration or solution absorption rate of salt or salt solution. The mass and heat balance within the air layer and the sorbent layer can be written as following.

Air layer ($\delta_s<z<\delta_s+\delta_a/2$):

$$\frac{\partial c_a}{\partial t} + u_a \frac{\partial c_a}{\partial x} - D_z \frac{\partial^2 c_a}{\partial z^2} = 0 \tag{S4}$$

$$\rho_a C_{p,a} \frac{\partial T_a}{\partial t} + u_a \rho_a C_{p,a} \frac{\partial T_a}{\partial x} - \lambda_a \frac{\partial T_a^2}{\partial y^2} = 0 \tag{S5}$$

Air-sorbent interface ($z=\delta_s$):

$$q_m\big|_{y=y0} = h_m(C_s - C_a), \quad q_T\big|_{y=y0} = h_T(T_s - T_a) \tag{S6}$$

Where the mass and heat transfer coefficients are, $h_m = D_z(2.0 + 0.6\,Re^{1/2}\,S\,c^{1/3})/\delta_a$ and $h_T = \lambda_a(2.0 + 0.6\,Re^{1/2}\,Pr^{1/3})\,/\delta_a$.

Sorbent layer ($0<z<\delta_s$):

$$\frac{\partial c_s}{\partial t} - D_z\frac{\partial^2 c}{\partial z^2} + \frac{1-\varepsilon_s}{\varepsilon_s}\rho_s\frac{\partial q}{\partial t} = 0 \tag{S7}$$

$$\rho_s C_{p,s}\frac{\partial T_s}{\partial t} - \lambda_s\frac{\partial T_s^2}{\partial z^2} = \rho_s\frac{\partial q}{\partial t}\Delta h_r \tag{S8}$$

The linear driving force model (LDF) is used to describe the sorption rate, the reaction coefficient k_{LDF} (1/s) is gained from the sorption curves from Figure S17.

$$\frac{\partial q}{\partial t} = k_{LDF}(q_e - q) \tag{S9}$$

Plane of symmetry ($z=0$, $z=\delta_s+\delta_a/2$):

$$\frac{\partial c}{\partial y} = 0, \frac{\partial T}{\partial y} = 0 \tag{S10}$$

The initial condition:

$$c\big|_{t=0} = c_0, T\big|_{t=0} = T_0 \tag{S11}$$

Where c_a ($g\cdot m^{-3}$) and c_s ($g\cdot m^{-3}$) are the vapor concentration in air and sorbent layer, u_a ($m\cdot s^{-1}$) is the air velocity within air layer. q ($g\cdot g^{-1}$) is the water uptake of sorbent. ρ_a ($g\cdot cm^{-3}$) and ρ_s ($g\cdot cm^{-3}$) are the density of air and composite sorbent. $C_{p,a}$ ($J\cdot g^{-1}\cdot K^{-1}$) and $C_{p,s}$ ($J\cdot g^{-1}\cdot K^{-1}$) are specific heat of air and composite. ε_s is the porosity of the composite. λ_a ($W\cdot m^{-1}\cdot K^{-1}$) and λ_s ($W\cdot m^{-1}\cdot K^{-1}$) are the thermal conductivity coefficient of air and

sorbent. D_z ($m^2 \cdot s^{-1}$) is the axis diffusivity, which is the binary mass diffusivity of water vapor in the air, calculated as following [4]:

$$D_{H_2O-air}(T,P) = 1.758 \times 10^{-4} \frac{(T+273.15)^{1.685}}{P_0} \left(\frac{m^2}{s} \right) \quad \text{(S12)}$$

The mathematic model of STB was solved by COMSOL.

S4. Lab-scale sorption thermal battery device

We design and construct an experimental system to demonstrate the concept of thermal energy harvesting from humidity by lab-scale sorption thermal battery. It is mainly composed of a fan (30 W, 220 $m^3 \cdot h^{-1}$, 125 Pa), an electric heater, one sorption thermal battery unit, and temperature sensors (PT100 with temperature accuracy of 0.15 ºC), humidity sensors (TH110-PNA300 with temperature accuracy of 0.2 ºC and humidity accuracy of 2.0% RH) and velocity sensor (WD400 thermal anemometer, 0-5 $m \cdot s^{-1}$ with accuracy of 3%). Sorption thermal battery unit is layer-by-layer assembled by twelve aluminum sheets with thickness of 0.5 mm, and each aluminum sheet is coated with two GA composite sheets with thickness about 2 mm. The interval between aluminum sheets is maintained 3 mm for air flow. The procedures to assemble the graphene aerogel composite sheets include, firstly, we clean the Al sheet with ethanol; Then, we will evenly brush the milk white glue (840#, purchased from Wen Ding adhesive Co., Ltd., water-soluble and mainly composed of vinyl acetate, acrylic ester and ethylene, stable at -30-100 ºC) to the Al sheet; Secondly, the composite sheets, which are completely dried at 80 ºC for at least 2 h, are coated onto the Al sheet. Subsequently, the Al sheet coated

with composite sheets will be heated at 80 ºC for several hours. And the milk white glue will change to colorless.

The STB unit is placed in a rectangular channel fabricated by acrylic with thickness of 5 mm (δ_1). To further suppress heat loss, a thermal insulated cotton with thickness of 20 mm (δ_2) and thermal conductivity of 0.034 W·m^{-1}·K^{-1} (λ_{cotton}) is coated on the outside surface of acrylic layer. We have evaluated the heat loss based on the equation:

$$P_{loss} = \frac{T_{sorb} - T_{amb}}{\frac{\delta_1}{\lambda_{acry}} + \frac{\delta_2}{\lambda_{cot\,ton}} + \frac{1}{h_{conv}}} \cdot S_{ext} \quad \text{(S13)}$$

Where P_{loss} (W) is heat loss of STB unit. $T_{sorb} - T_{amb}$ (ºC) is the temperature difference between sorbent and ambient, h_{conv} $(W \cdot m^{-2} \cdot K^{-1})$ is the convective heat transfer coefficient at the surface of insulated cotton, S_{ext} (m^2) is the external surface of STB.

The heat loss P_{loss} is less than 2 W and thus it is ignored in the energy analysis. In addition, we use the LFA Thermal Analyzer to gain the thermal conductivity of GA matrix is 0.037 W·m^{-1}·K^{-1} and the thermal conductivity of GA composite ($CaCl_2$@GA) is 0.19 W·m^{-1}·K^{-1}. When air flows through the sorbent layer, the efficient convective heat transfer between air and sorbent as well as the heat transfer within the thin sorbent layer can ensure the efficient heat transfer ability of STB.

The working cycles of this prototype include the charging and discharging processes. In the charging process, air with a flow rate about 72 m^3·h^{-1} is heated to 50 ºC/80 ºC by an electrical heater. When hot air passes thorough sorption thermal battery, water in

$CaCl_2$@GA composite sorbents will be released and taken away by air flow. When the temperature difference decreases below 3 ºC, the charging process is regarded as finished. In the discharging process, high humidity ambient is preferential, when cold humidity air with a flow rate about 36 $m^3 \cdot h^{-1}$ passes through sorption thermal battery, vapor will diffuse into the $CaCl_2$@GA composite sorbents and be captured by salt or salt solution within the GA matrix. The sorption heat will heat the cold air to get warm air to supply heat to indoor temperature control. When temperature lift is less than 3 ºC, the discharging stage is regarded as finished.

Due to good heat transfer between air and the composite sorbent, the air temperature and the sorbent is assumed to be locally in thermal equilibrium. Therefore, in a steady state, the sorption heat is completely used to heat the moist air. Hence, the relation of temperature and humidity can be given as: [5]

$$(d_o - d_i) \cdot \Delta h_r^0 = C_{p,g} \cdot (T_i - T_o) \tag{S14}$$

$$\frac{T_i - T_o}{d_o - d_i} = \frac{\Delta h_r^0}{C_{p,air}} \tag{S15}$$

Where d_i *and* d_o ($g \cdot kg^{-1}$) are the input and output moisture content, T_i (ºC) and T_o (ºC) are the input and output temperature, Δh_r^0 ($J \cdot g^{-1}$) is the adsorption heat per gram water. $C_{p,air}$ ($J \cdot K^{-1} \cdot g^{-1}$) is the specific heat of air.

The instantaneous charging or discharging power can be calculated on the temperature difference or the absolute humidity change.

$$P_c = Q_m \cdot C_{p,air} \cdot (T_i - T_o) = Q_m \cdot \Delta h_r^0 \cdot \left(d_o - d_i\right) \tag{S16}$$

$$Q_c = \int_0^{t_c} Q_m \cdot C_{p,air} \cdot (T_i - T_o)dt = \int_0^{t_c} Q_m \cdot \Delta h_r^0 \cdot (d_o - d_i)dt \tag{S17}$$

$$P_d = Q_m \cdot C_{p,air} \cdot (T_o - T_i) = Q_m \cdot \Delta h_r^0 \cdot \left(d_i - d_o\right) \tag{S18}$$

$$Q_d = \int_0^{t_d} Q_m \cdot C_{p,air} \cdot (T_o - T_i)dt = \int_0^{t_d} Q_m \cdot \Delta h_r^0 \cdot (d_i - d_o)dt \tag{S19}$$

Where, P_c (W) and P_d (W) are the charging and discharging power, Q_c (J) and Q_d (J) are the charging and discharging heats of STB. Q_m (g·s^{-1}) is the mass flow rate of air, which is calculated by $Q_m = S \cdot V_{in} \cdot \rho_{air}$, S (m^2) is the sectional area of the air channel, ρ_{air} (kg·m^{-3}) is the air density, *Vin* (m·s^{-1}) is the air velocity within the air channel.

$$q_{ad} = \frac{m_{a,H_2O}}{m_{sorb,dried}} = \frac{1}{m_{sorb,dried}} \cdot \int_0^{t_a} Q_m \cdot (d_i - d_o)dt \tag{S20}$$

$$PD_m = \frac{P_d}{m_{sorb,dried}}, \quad PD_V = \frac{\rho_{sorb,dried} \cdot P_d}{m_{sorb,dried}} \tag{S21}$$

$$ED_m = \frac{Q_d}{m_{sorb,dried}}, ED_V = \frac{\rho_{sorb,dried} \cdot Q_d}{m_{sorb,dried}} \tag{S22}$$

$$\eta = \frac{Q_d}{Q_c} \tag{S23}$$

Where q_{ad} (g·g^{-1}) is the water uptake captured by composite during adsorption process (charging stage), $m_{sorb,dried}$ (g) is the mass of graphene aerogel composite in dried state and $m_{a,H2O}$ (g) is the mass of captured water by graphene aerogel composite. PD_m (W·kg^{-1}), PD_V (W·m^{-3}) are the mass specific power and the volume specific power. ED_m (Wh·kg^{-1}), ED_V (Wh·m^{-3}) are the mass storage density and volume storage density.

The uncertainties can be calculated by the following equations.

$$\left|\frac{\delta V_i}{V_i}\right| = 3\%,\ \left|\frac{\delta T_i}{273.15+T_i}\right| = 0.05\%,\ \left|\frac{\delta T}{T_o - T_i}\right| = 1.5 \sim 5\%,\ \left|\frac{\delta RH}{RH}\right| = 2\%,\ \left|\frac{\delta d}{d}\right| \approx 2\%,$$

$$\left|\frac{\delta d}{d_0\text{-}d_i}\right| \approx 6\sim 30\%$$

$$\frac{\delta Q_m}{Q_m} = \left|\frac{\delta V_i}{V_i}\right| + \left|\frac{\delta T_i}{273.15+T_i}\right| \approx 3\%$$

$$\left|\frac{\delta P}{P}\right| = \left|\frac{\delta Q_m}{Q_m}\right| + \left|\frac{\delta T}{T_0 - T_i}\right| \approx 4.5 \sim 8\%$$

$$\left|\frac{\delta q_{ad}}{q_{ad}}\right| = \left|\frac{\delta Q_m}{Q_m}\right| + \left|\frac{\delta d}{d_0 - d_i}\right| \approx 10.5 \sim 33\%$$

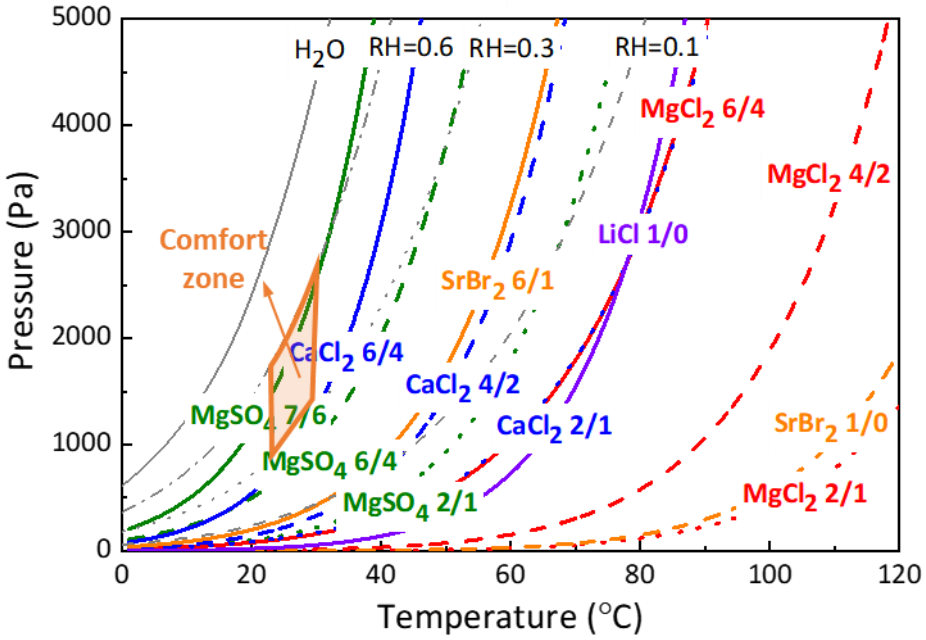

Figure S1. Equilibrium curves of different salt hydrates for climate control, thermodynamics data based on Donkers[6]

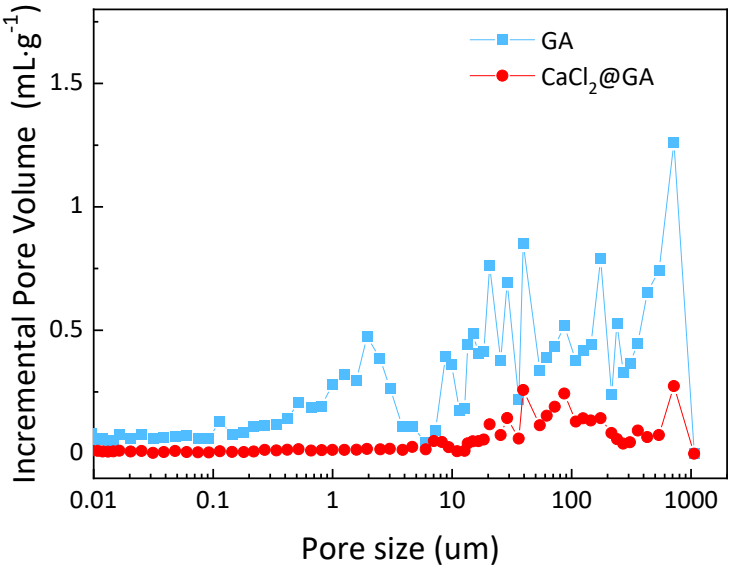

Figure S2. The pore size distribution of GA matrix and $CaCl_2$@GA, obtained by mercury intrusion method

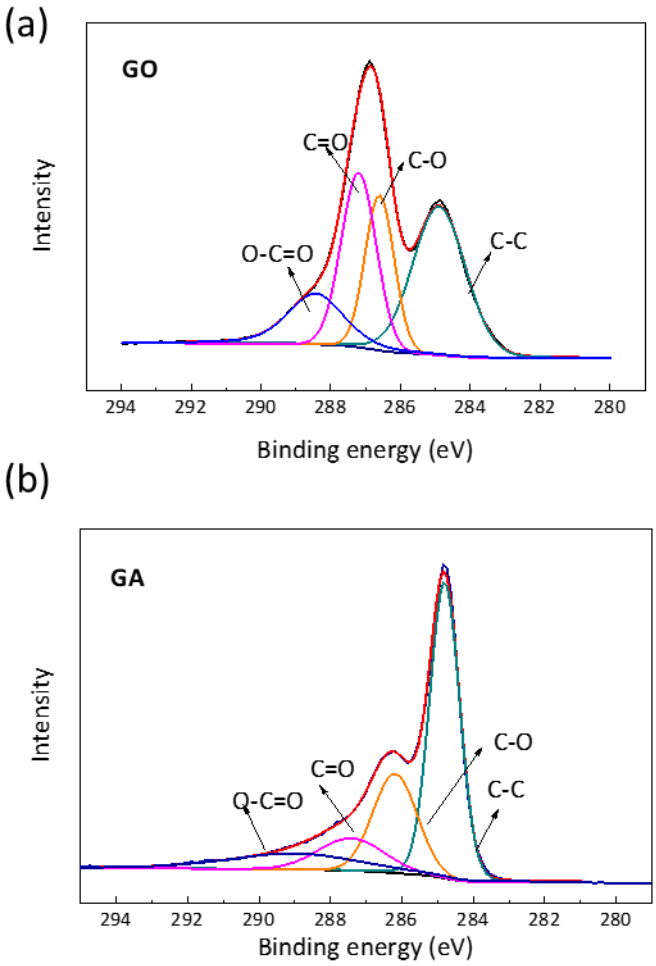

Figure S3. C1s X-ray photoelectron spectra for (a) graphene oxide, (b) graphene aerogel

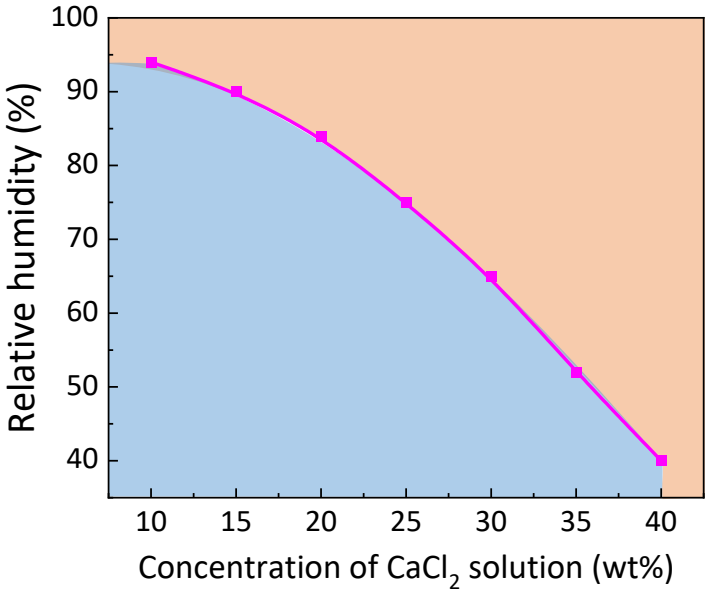

Figure S4. Equilibrium concentration of $CaCl_2$ solution (line) at different RHs

Figure S5. Digital images of graphene hydrogels with different sizes

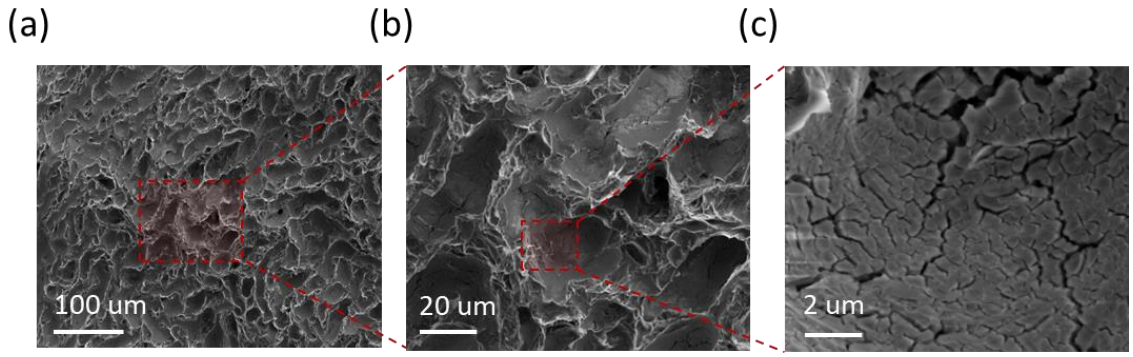

Figure S6 SEM images of $CaCl_2$@GA_30

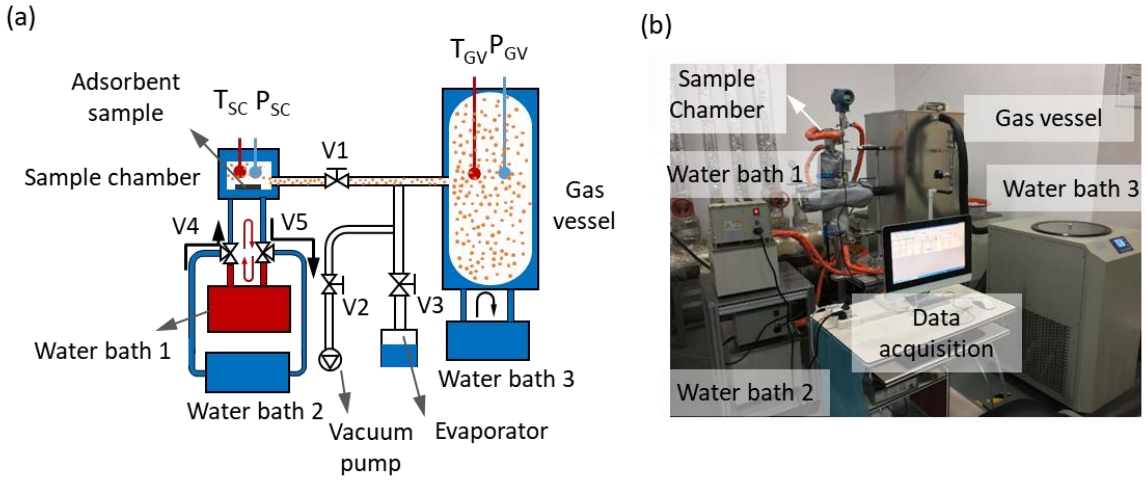

Figure S7. Schematic diagram of self-building sorption device. It is mainly composed of gas vessel, sample chamber and evaporator. The sorption temperature is controlled by water bathes, and the vapor is stored in the gas vessel, the vapor pressure is regulated by the evaporator, a vacuum pump is used to degas the air within the reactor, and temperature and vapor pressure of the sample chamber and gas vessel is recorded by the data acquisition system.

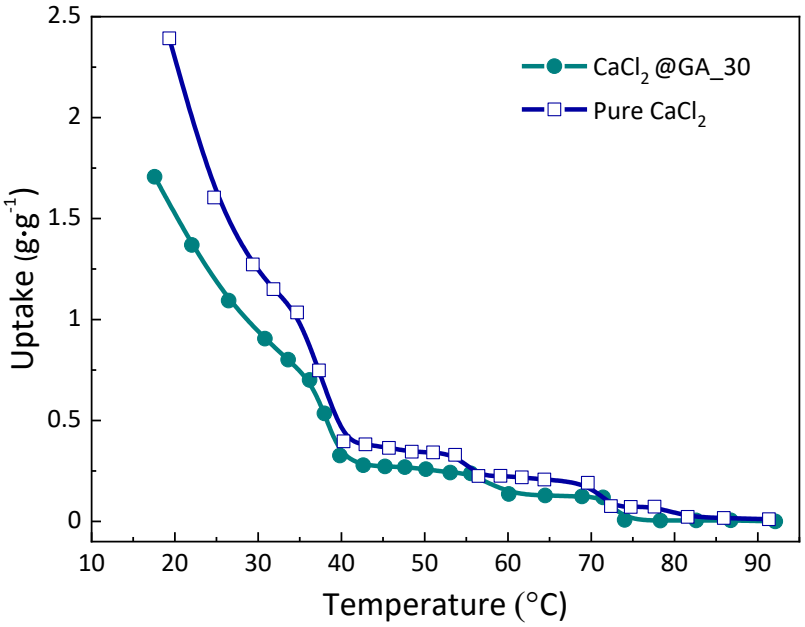

Figure S8. Isobaric sorption equilibrium curves of pure $CaCl_2$ and $CaCl_2$@GA_30 at 1200Pa

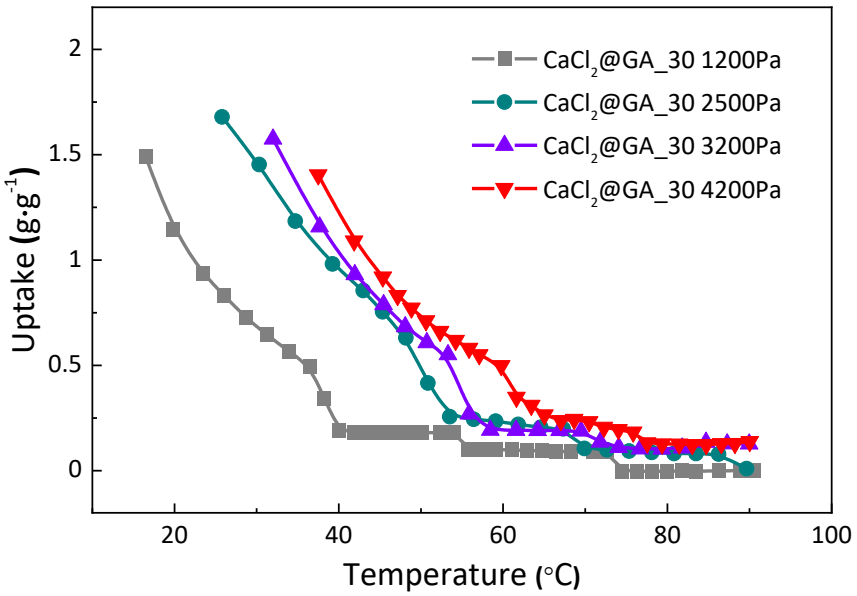

Figure S9. Isobaric equilibrium curves of $CaCl_2$@GA_30 at different pressures

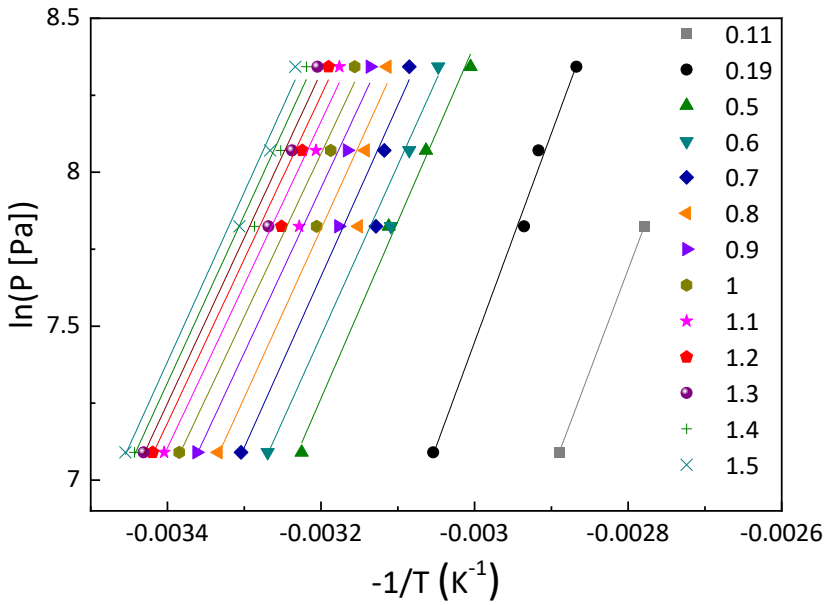

Figure S10. Ln (P) vs. -1/T at different water uptake showing water sorption/desorption equilibrium characteristic of $CaCl_2$@GA_30

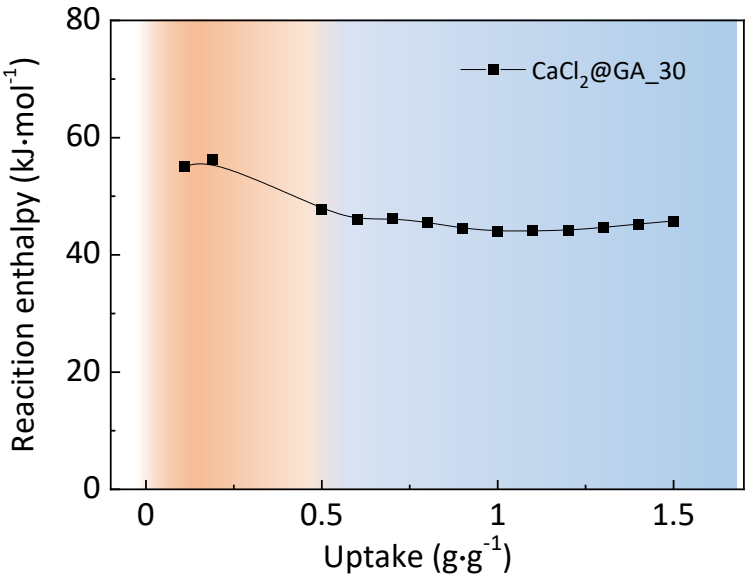

Figure S11. The reaction enthalpy of $CaCl_2$@GA composite sorbent per mole of water at different water uptakes

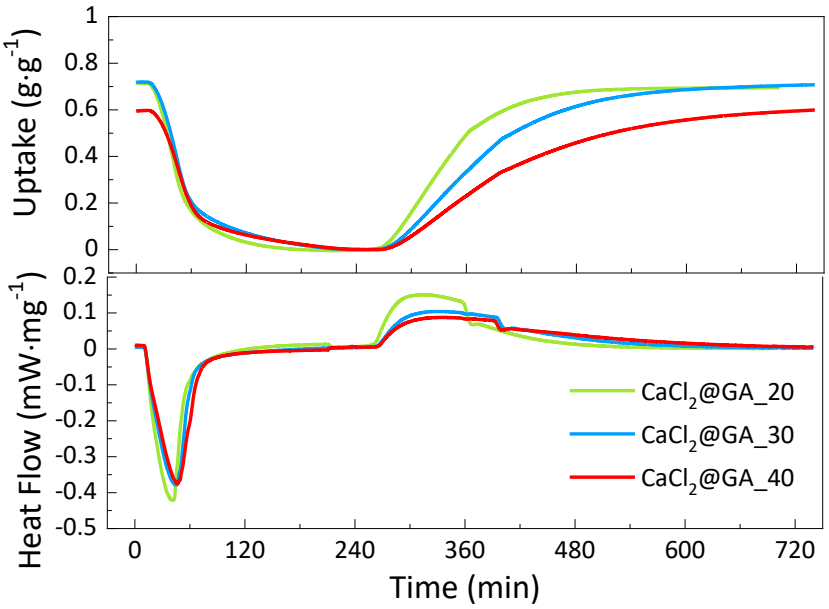

Figure S12. TG-DSC curves of $CaCl_2$@GA_20/30/40 sorbents sorption under 30% RH at 30 ºC and desorption at 80 ºC

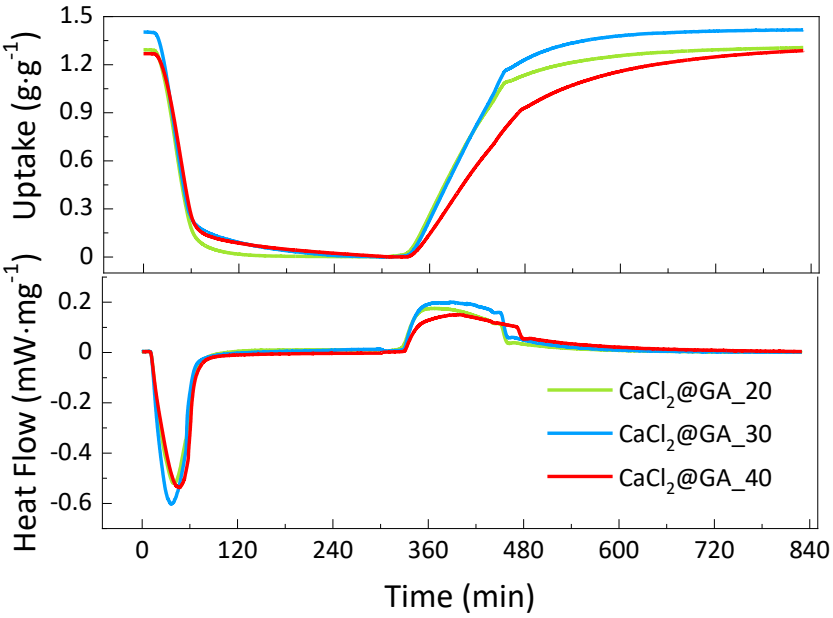

Figure S13. TG-DSC curves of $CaCl_2$@GA_20/30/40 sorbents sorption under 60% RH at 30 ºC and desorption at 80 ºC

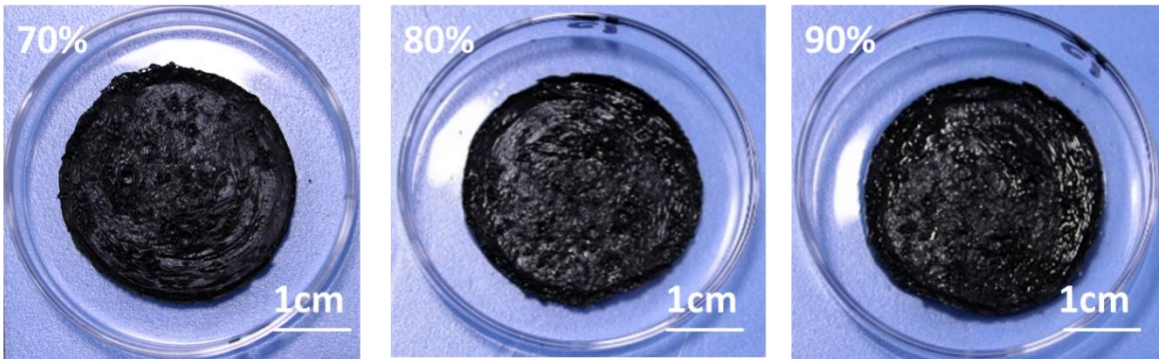

Figure S14. Digital images of $CaCl_2$@GA_30 under different humidity conditions

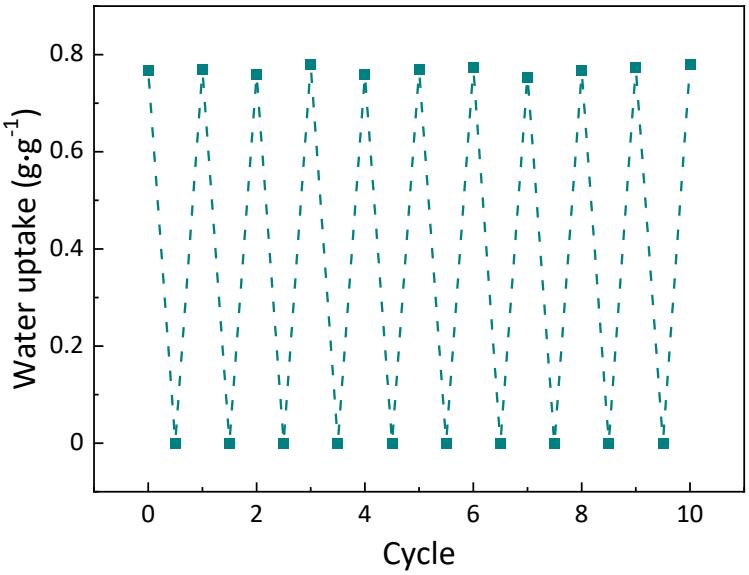

Figure S15. Cycling stability evaluation of $CaCl_2$@GA_30 (sorption condition: 30% RH at 30 ºC; desorption condition: 2.5% RH at 80 ºC)

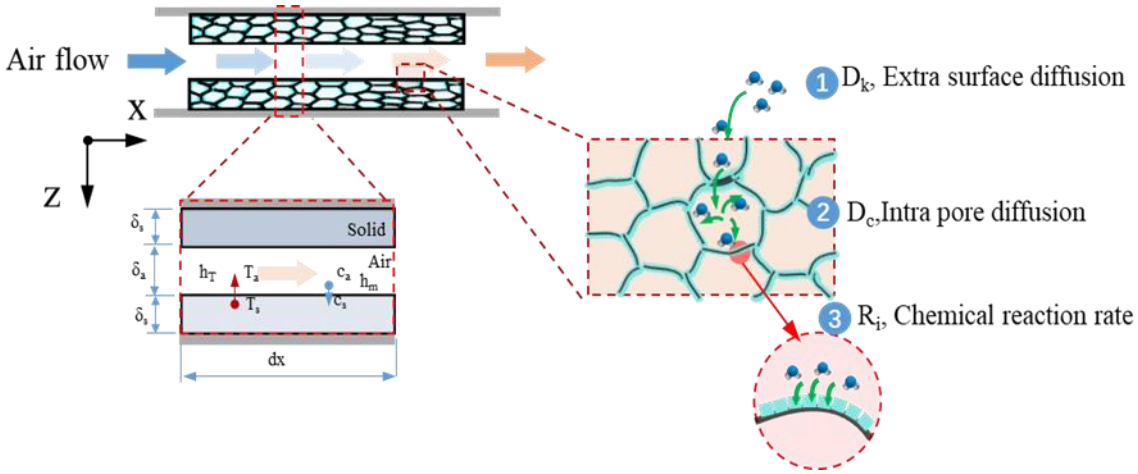

Figure S16. Water vapor mass diffusion and heat transfer within $CaCl_2$@GA composite sorbent

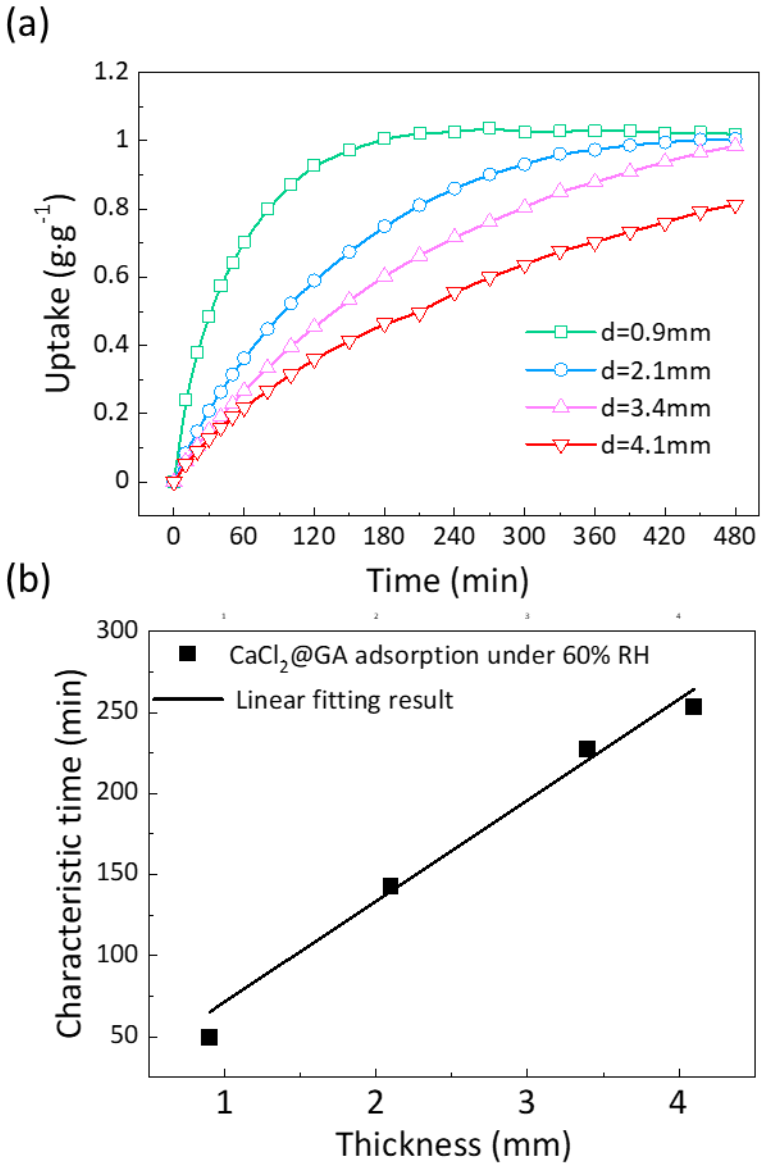

Figure S17. (a)Water sorption curves at 30 ºC RH 60% of $CaCl_2$@GA_30 at different sorbent thicknesses. (b) Sorption characteristic times change with sorbent thickness

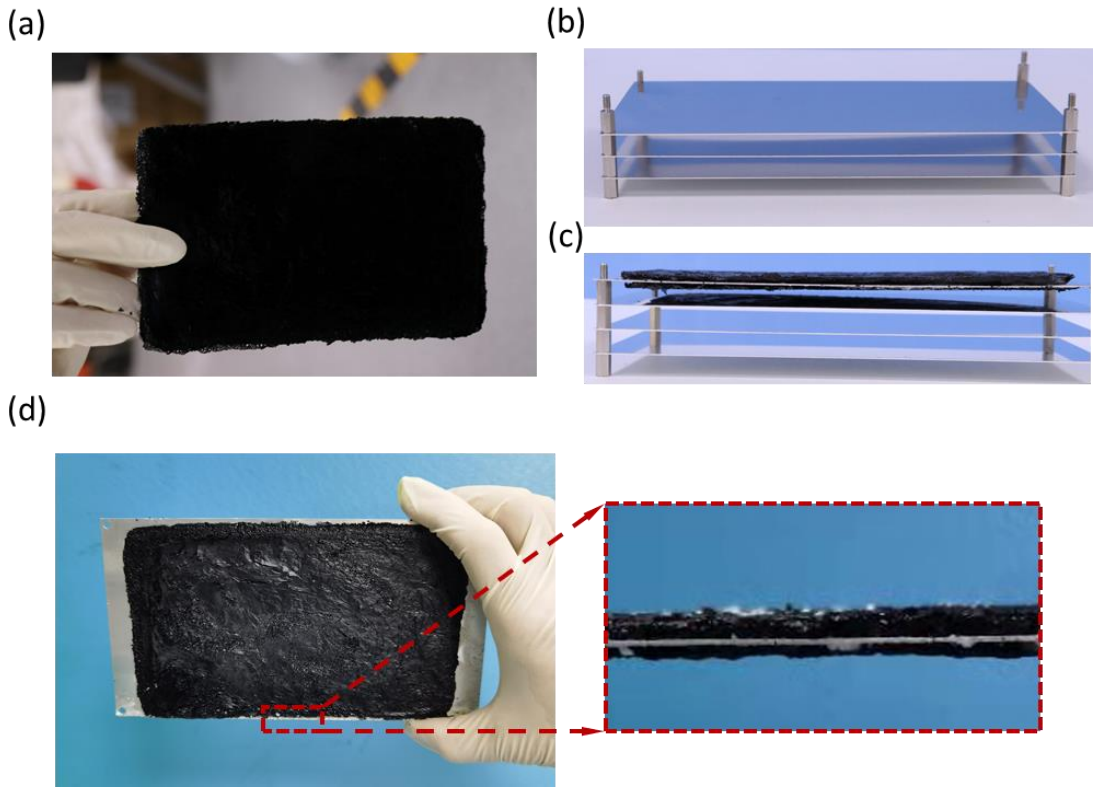

Figure S18 The images of (a) $CaCl_2$@GA composite sorbent sheet, (b) aluminum sheets, (c) the layer-by-layer assembly for STB by the composite sorbent coated at the two sides of aluminum sheets and (d) the coated composite sorbent onto the aluminum sheets after dozens of repeated charging/discharging cycles

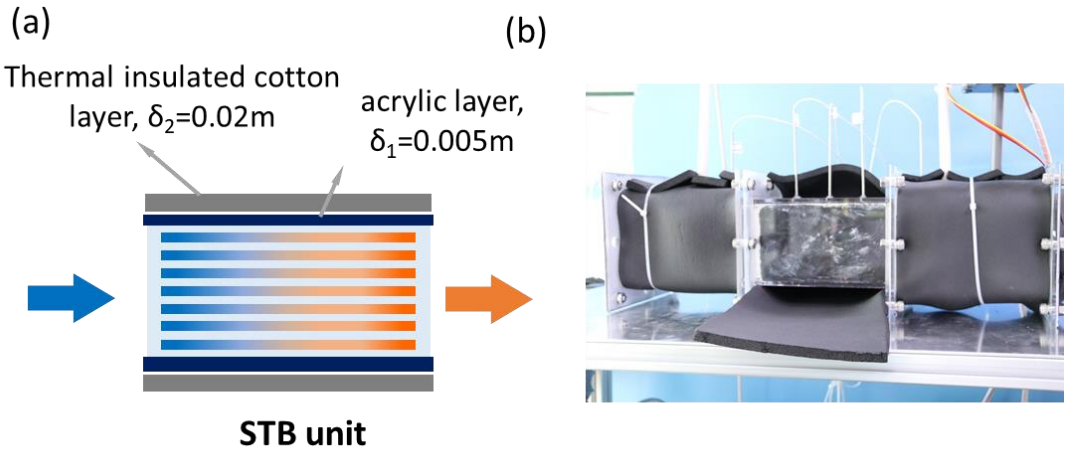

Figure S19 (a) The STB envelope structure and (b) Optical photograph of the STB unit with thermal insulation for suppress heat loss.

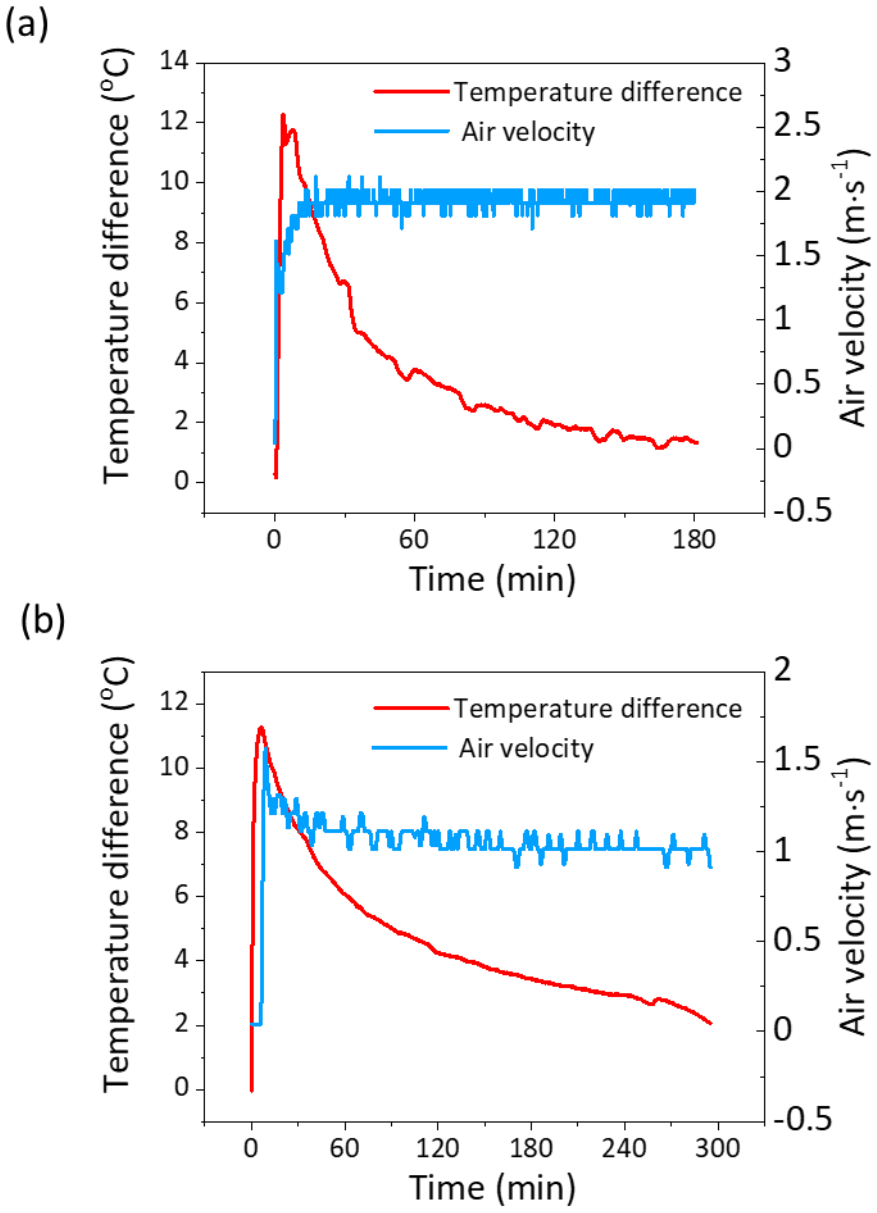

Figure S20. Temperature difference and air flow velocity during (a) charging stage (desorption) and (b) discharging stage (sorption)

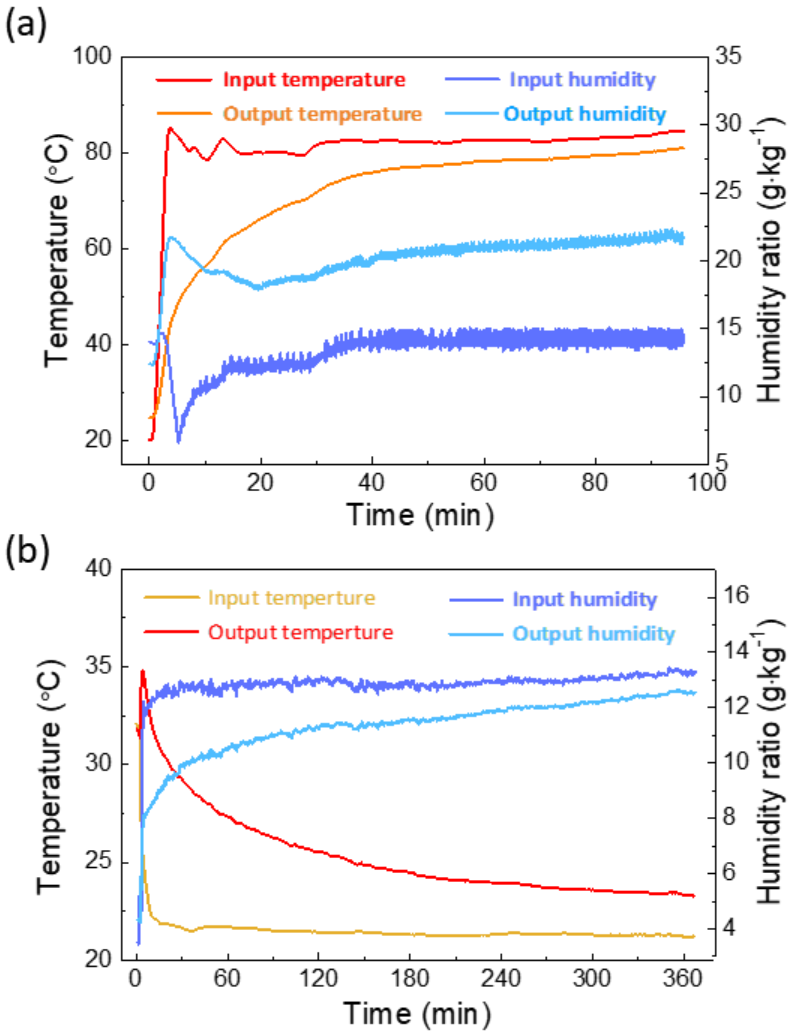

Figure S21. (a) Temperature and humidity evolutions of the STB during thermal charging process at driving temperature of 80 ºC. (b) Temperature and humidity evolutions of the STB during thermal discharging process at 20 ºC under 80% RH.

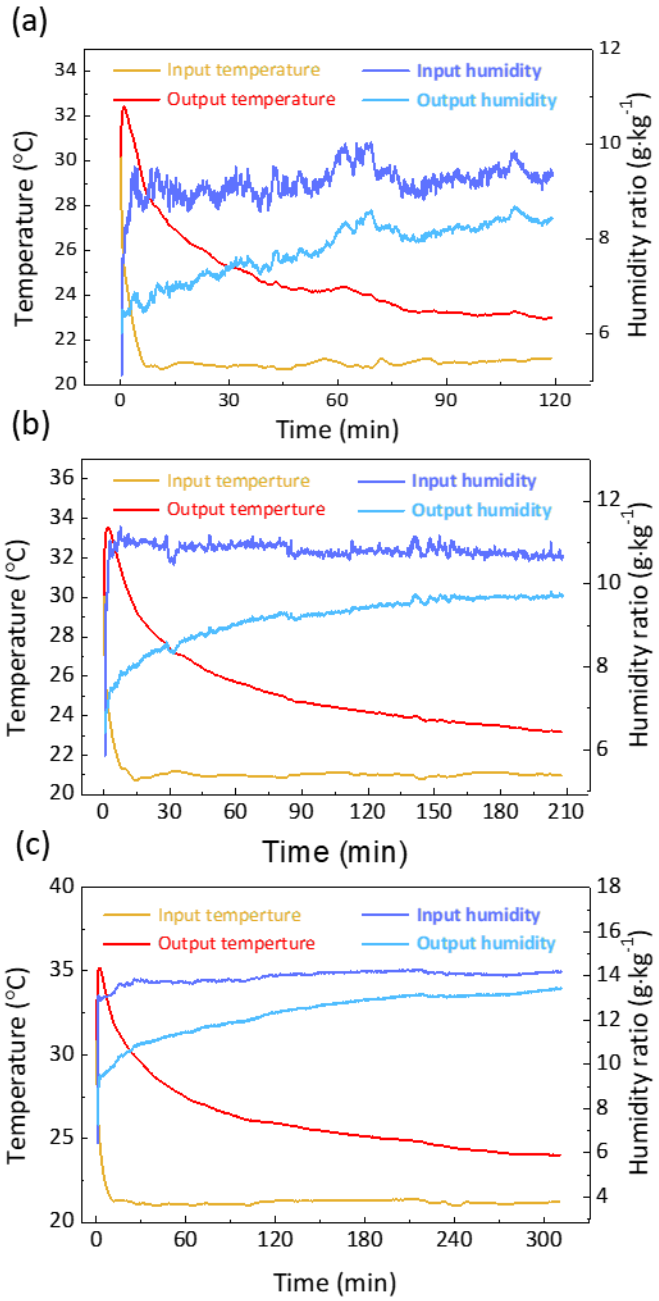

Figure S22. Temperature and humidity evolutions of the STB during thermal discharging process at 20 ºC under (a) 60% RH, (b).70% RH and (c) 90% RH

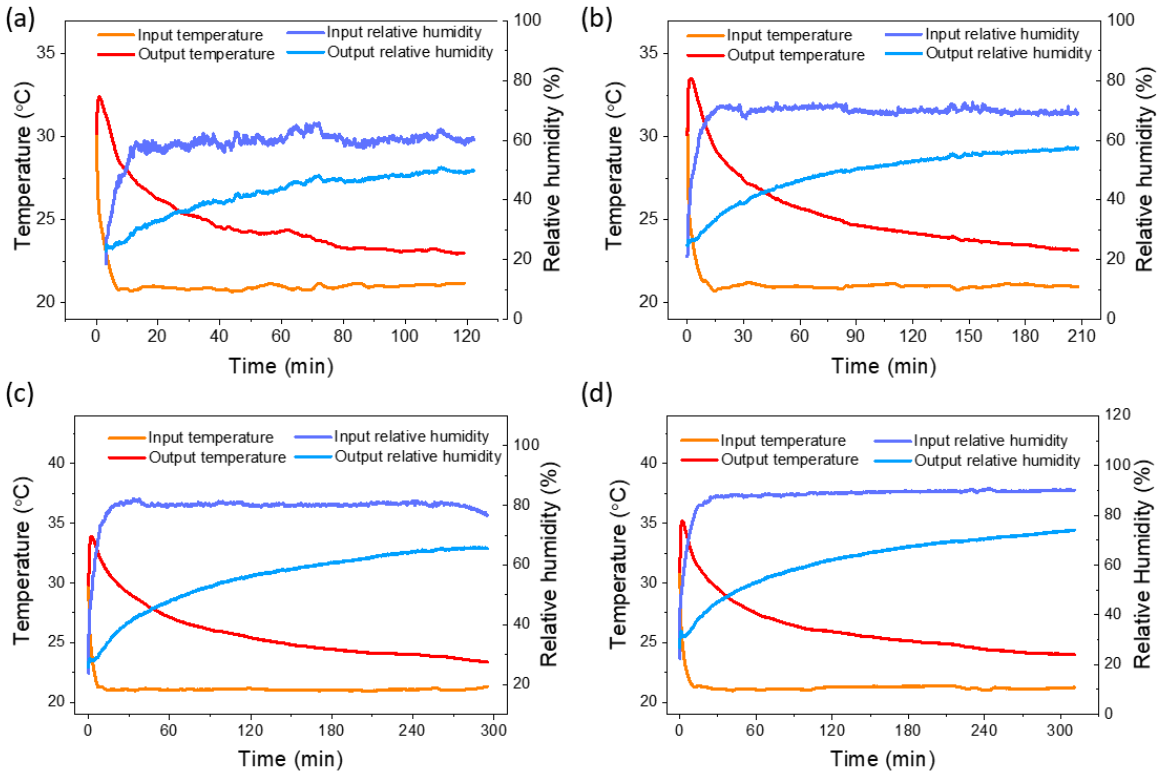

Figure S23. Temperature and relative humidity evolutions of the STB during thermal discharging process at 20 ºC under (a) 60% RH, (b)70% RH, (c) 80% RH and (d) 90% RH

Table S1. Salt loaded and packed density of $CaCl_2$@GA composite sorbents with different salt concentrations

Sample	Concentration of $CaCl_2$ solution, wt%	Theoretic density, g.cm^{-3}	Real packed density, g.cm^{-3}	Salt loading, wt%	Maximum uptake without leakage, g·g^{-1}
$CaCl_2$@GA_20	20	0.28	0.25±0.02	91.6	4.17
$CaCl_2$@GA_30	30	0.45	0.36±0.05	94.2	2.80
$CaCl_2$@GA_40	30	0.64	0.59±0.06	96.4	1.66

Generally, the density of graphene aerogel composite increases with the increase of salt loading, what's more, as the density of aerogel matrix is extremely low, the salt loading is typically larger than 90%. The salt loading and maximum water uptake are calculated by the following equations,

$$\rho_{theo,c} = \rho_{GA} + \varepsilon \cdot \rho_{CaCl_2,sol} \cdot c_{CaCl_2} \tag{S24}$$

$$\gamma_{salt} = 1 - \rho_{GA} \Big/ \rho_{c,dried} \tag{S25}$$

$$q_{\max} = \frac{\varepsilon \cdot \rho_{CaCl_2,sol,f}}{\rho_{c,dried}} \tag{S26}$$

Where $\rho_{theo,c}$ (g·cm^{-3}) is the theoretic density of GA composite, c_{CaCl_2} (wt%) is mass ratio of $CaCl_2$ for the $CaCl_2$ solution used for wet impregnation. $\rho_{CaCl_2,sol}$ (g·cm^{-3}) is the density of $CaCl_2$ solution. ε (%) is the porosity of GA. ρ_{GA} (g·cm^{-3}) *and* $\rho_{c,dry}$ (g·cm^{-3}) are the density of GA and composite sorbent in dried state. γ_{salt} (wt%) is the salt content within GA matrix in weight. $\rho_{CaCl_2,sol,f}$ (g·cm^{-3}) is the density of $CaCl_2$ solution formed at the maximum water uptake. q_{max} (g·g^{-1}) is the maximum uptake without leakage for as-fabricated composite.

Table S2. Water sorption performance of the $CaCl_2$@GA composite sorbents gained by TG-DSC

Sample	T_{ad}, °C	Humidity, %	T_{de}, °C	Water uptake, $g \cdot g^{-1}$
$CaCl_2$@GA_20	30	30	80	0.70
		60	80	1.29
$CaCl_2$@GA_30	30	30	80	0.76
		60	80	1.4
$CaCl_2$@GA_40	30	30	80	0.76
		60	80	1.21

Table S3. Performance comparison in terms of the salt loading, water uptake and energy density between the $CaCl_2$@GA and the reported sorbents with different salts and porous matrices for thermal storage applications

Porous matrix	Salt	Salt loading (wt%)	Sorption Temperature (°C)	Sorption pressure (Pa)	Desorption Temperature (°C)	Water uptake ($kg \cdot kg^{-1}$)	Energy density ($kJ \cdot kg^{-1}$)	Ref.
MIL-101(Cr)	$CaCl_2$	62	30	1250	80	0.58	1746	[7]
UiO-66	$CaCl_2$	58	30	2360	110	0.63	-	[8]
Alginate-derived polymeric matrix	$CaCl_2$	76	30	1270	130	0.88	1206	[9]
	$MgCl_2$	81	30	1270	150	0.93	1018	
MWTCNT	LiCl	44	35	870	75	0.57	1700	[10]
Silicate gel	LiCl	43.6	35	810	80	-	1159	[11]
Silicate gel	$SrBr_2$	58	30	1250	80	0.22	828	[12]
Zeolite	$MgSO_4$	15	30	1590	150	0.15	648	[13]
Zeolite	$MgCl_2$	12.6	30	2500	200	0.26	842	[14]
Vermiculite	LiCl	59	35	870	75	0.6	1800	[15]
GA	$CaCl_2$	96	30	1250	80	0.76	1841	This work
			30	3796	80	2.89	7768	

Table S4. Basic specific characteristics of lab-scale sorption thermal battery using $CaCl_2$@GA composite sorbent

	Value	Unit		Value	Unit
Sorbent	$CaCl_2$@GA		Thickness of sorbent	2.0±0.5	mm
Sorbent Mass	240.2	g	Thickness of Al-fins	0.5	mm
Mass of Al-sheets	306.5	g	Interval of sorbent sheets	3.4±0.7	mm
Total Mass	546.7	g	Flow area of reactor	100	cm^2
Density of sorbent	0.33	$g \cdot cm^{-3}$	Length of reactor	18	cm
Volume of sorbent	740	cm^3	Total volume	1800	cm^3

Table S5. Performance of sorption thermal battery

	Case 01	Case 02	Case 03	Case 04	Case 05
Input temperature, ºC	21	21	21	21	21
Input relative humidity, %	59.4	69.7	80.1	80.1	90.4
Rate of air flow during discharging, $m^3 \cdot h^{-1}$	36	36	36	36	36
Charging temperature, ºC	50	50	50	80	50
Rate of air flow during charging, $m^3 \cdot h^{-1}$	72	72	72	72	72
Maximum charging power, W	238.7	310	290.6	626.9	328.1
Average charging power, W	58.7	54.2	88.5	163.7	98.5
Maximum discharging power, W	134.3	137.2	152.4	133.8	195.7
Average discharging power, W	48.7	47.2	53.7	49.6	55.7
Maximum discharging power density, $W \cdot kg^{-1}$	559	572	635	556	815
Charged capacity, kWh	0.13	0.159	0.286	0.33	0.42
Discharged capacity, kWh	0.10	0.13	0.23	0.24	0.38
Mass energy storage density, $Wh \cdot kg^{-1}$	402	525	950	992	1580
Volume storage density, $kWh \cdot m^{-3}$	131	171	309	323	514
Water capacity, $g \cdot g^{-1}$	0.55	0.71	1.28	1.22	1.74
Storage efficiency	0.73	0.80	0.80	0.60	0.90

References

(1) Xu, Y.; Sheng, K. X.; Li, C.; Shi. G. Q. Self-Assembled Graphene Hydrogel via a One-Step Hydrothermal Process. *ACS Nano* **2010**, *4*, 4324-4330.

(2) Chen, W.; Yan, L. In situ Self-assembly of Mild Chemical Reduction Graphene for Three-Dimensional Architectures. *Nanoscale* **2011**, *3*, 3132-313.

(3) Yang, H. S.; Li, Z. L.; Lu, B.; Gao, J.; Jin, X. T.; Sun, G. Q.; Zhang, G. F.; Zhang, P. P.; Qu, L. T. Reconstruction of Inherent Graphene Oxide Liquid Crystals for Large-Scale Fabrication of Structure-Intact Graphene Aerogel Bulk toward Practical Applications. *ACS Nano* **2018**, *11*, 11407-11416

(4) Sharafian, A.; Bahrami, M. Adsorbate Uptake and Mass Diffusivity of Working Pairs in Adsorption Cooling Systems. *Int. J. Heat Mass Transf.* **2013**, *59*, 262-271.

(5) Marias, F.; Neveu, P.; Tanguy, G.; Papillon P. Thermodynamic Analysis and Experimental Study of Solid/Gas Reactor Operating in Open Mode. *Energy* **2014**, *66*, 757-765.

(6) Donkers, P. A. J.; Sögütoglu, L. C.; Huinink, H. P.; Fischer, H. R.; Adan, O. C. G. A Review of Salt Hydrates for Seasonal Heat Storage in Domestic Applications. *Appl. Energy* **2017**, *199*, 45-68.

(7) Permyakova, A.; Wang, S.; Courbon, E.; Nouar, F.; Heymans, N.; D'ans, P.; Barrier, N.;Billemont, P.; De Weireld, G.; Steunou, N.; Frère, M.; Serre, C. Design of Salt–

Metal Organic Framework Composites for Seasonal Heat Storage Applications. *J. Mater. Chem. A* **2017**, *5*, 12889-12898.

(8) Garzón-Tovar, L.; Pérez-Carvajal, J.; Imaz, I.; Maspoch, D. Composite Salt in Porous Metal-Organic Frameworks for Adsorption Heat Transformation. *Adv. Funct. Mater.* **2017**, *27*, 1606424.

(9) Kallenberger, P. A.; Posern, K.; Linnow, K.; Brieler, F. J.; Steiger, M.; Fröba, M. Alginate-Derived Salt/Polymer Composites for Thermochemical Heat Storage. *Adv. Sustainable Systems* **2018**, *2*, 1700160.

(10) Gordeeva, L. G.; Grekova, A. D.; Aristov, Yu. I. Composites "Li/Ca Halogenides inside Multi-Wall Carbon Nano-Tubes" for Adsorptive Heat Storage, *Sol. Energy Mater. Sol. Cells*, **2016,** *155*, 176-183.

(11) Yu, N.; Wang, R. Z.; Lu, Z. S.; Wang, L. W. Development and Characterization of Silica Gel–LiCl Composite Sorbents for Thermal Energy Storage. *Chem. Eng. Sci.* **2014**, *111*, 73-84.

(12) Courbon, E.; D'Ans, P.; Permyakova, A.; Skrylnyk, O.; Steunou, N.; Degrez, M.; Frère, M., A New Composite Sorbent Based on $SrBr_2$ and Silica Gel for Solar Energy Storage Application with High Energy Storage Density and Stability. *Appl. Energy* **2017**, *190*, 1184-1194.

(13) Hongois, S.; Kuznik, F.; Stevens, P. and Roux, J.-J. Development and

Characterisation of a New $MgSo_4$−Zeolite Composite for Long-Term Thermal Energy Storage. *Sol. Energy Mater. Sol. Cells* **2011**, *95*, 1831-1837.

(14) Yan, T. S.; Li, T. X.; Xu, J. X. and Wang, R. Z. Water Sorption Properties, Diffusion and Kinetics of Zeolite NaX Modified by Ion-Exchange and Salt Impregnation. *Int. J. Heat Mass Transf.* **2019**, *139*, 990-999.

(15) Grekova, A. D.; Gordeeva, L. G.; Aristov, Y. I., Composite "LiCl/Vermiculite" as Advanced Water Sorbent for Thermal Energy Storage. *Appl. Therm. Eng.* **2017**, *124*, 1401-1408.